Proceedings of 20th International Congress on Acoustics, ICA 2010

23-27 August 2010, Sydney, Australia

Modelling coherent elastic wave propagation through creep damaged material

Mihai Caleap, Bruce W. Drinkwater and Paul D. Wilcox

Department of Mechanical Engineering, University of Bristol, Queens Building, University Walk, Bristol BS8 1TR, UK

PACS: 43.20.Bi, 43.20.Fn, 43.20.Hq, 43.35.Cg

ABSTRACT

In this paper, a creep-damaged material is modelled as a two-phase composite material comprising a matrix and a distribution of clustered spherical voids. The voids are dispersed uniformly within oblate ellipsoidal regions that represent preferred regions of voiding close to grain boundaries. In turn, the ellipsoidal regions are distributed randomly in the matrix. A double composite model based on coherent elastic wave propagation is used to determine the effective stiffness and the overall density of the two-phase material. As the creep progresses, the ellipsoid elements are sparsely scattered in the matrix, but they continue to grow in volume, containing more and more voids within them. This evolution results in an anisotropy increase due to the preferential void formation within the ellipsoid elements. Velocity estimates can be used to predict the elastic softening and the development of anisotropy, providing bulk-average information pertinent to the assessment of creep damage.

INTRODUCTION

Problems involving the modelling of wave propagation in particulate composites are generally recognized as being impossible to solve analytically. This is because infinite orders of rescattering have to be considered along with the need to satisfy the continuity conditions for stresses and displacements across each of the cavity boundaries when, in many cases, the exact location of each of the cavities (with respect to some chosen origin) is unknown.

Often, however, the analysis can be simplified by replacing the composite medium by a homogeneous *effective* medium that can be characterized by an appropriate choice of effective static and dynamic parameters (*e.g.*, wavenumber, elastic moduli, density, etc.). For a low concentration of sparsely distributed scatterers, when multiple scattering effects are negligible, single scattering approaches can often be used reliably. If the dimensions of the cavities are sufficiently small so that thir resonant frequencies lie outside the frequency band of interest, then models, such as that of Kuster and Toksöz [1], can be employed. Many other homogenisation schemes have been proposed to obtain the effective elastic properties of particulate composites, see *e.g.* [2-5]. In particular, optimal bounds in which the effective moduli must reside were developed [6]. For higher concentrations of scatterers, multiple scattering approaches can also be used, for example, that of Waterman and Truell [7] which accounts for the first order of rescattering but not higher orders, or that developed more exactly by Varadan *et al.* [8] in which the effective wavenumbers in the low frequency limit are obtained from simple dispersion relations.

In effect, all of these models provide a means of obtaining a set of frequency-dependent estimates for effective parameters (*e.g.*, wavenumber, elastic moduli, density, etc.) as a function of the material properties of the constituent media, the dimensions of the cavities, and the void fraction.

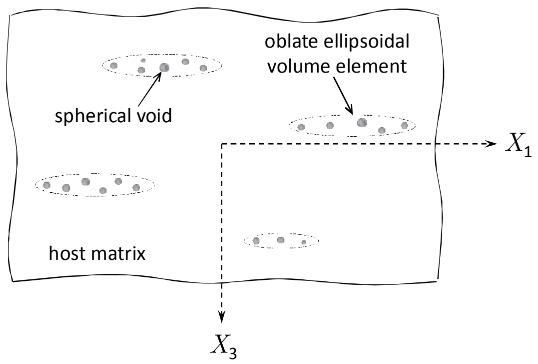

Figure 1. Two-dimensional sketch of double composite modelling for intergranular creep process.

The present paper is concerned only with the modelling of elastic wave propagation through the various types of void-filled media in the low-frequency limit (long wavelength compared with the lengthscale of the microstructure of the composite). Enhancements to allow modelling in higher frequency regions is the subject of on-going research. Further, since effective medium techniques are now well established for simple shaped and uniformly distributed cavities and elastic inclusions, the work concentrates on their application to creep-damaged materials.

We consider creep damage in a metal to result in a two-phase composite material comprising an isotropic matrix and spherical voids. The voids are assumed to be dispersed uniformly within oblate ellipsoidal regions (or volume elements). The volume elements are randomly distributed in the matrix. A two-dimensional sketch of this *double composite material* is illustrated in Figure 1. The calculation procedure with this model consists of two steps. First, the spherical voids are assumed to be randomly and uniformly distributed in the matrix. We calculate the effective stiffness and the overall density of the *porous material*. Second, the oblate ellipsoidal inclusions, whose density and stiffness are known from the previous step, are distributed randomly in the matrix with the minor axes parallel to the stress direction, and the new effective stiffness is obtained. This model allows us to determine the effective velocities of the coherent elastic waves propagating and polarized in the principal directions of the transverse isotropy. The present treatment draws much on previous work by many researchers, especially of Ledbetter *et al.* [9] and Jeong and Kim [10]. For simplicity, we assume that the effective velocities are affected only by the creep voids.

POROUS MATERIAL

Suppose that identical spherical cavities of radius a are distributed randomly and uniformly in an isotropic homogeneous elastic solid. The concentration of cavities is denoted by ϕ_0. In view of the coherent elastic wave propagation with frequency ω, the given medium may be seen as isotropic homogeneous made up of some effective material. Let ρ_0, κ_0 and μ_0 denote respectively, the mass density, the bulk modulus and the shear stiffness of the matrix material. The density ρ_*, the bulk modulus κ_* and the shear stiffness μ_* of the effective material depend on the concentration ϕ_0 and on the scattering dispersion parameter

$$\tilde{\omega}_w = k_w a\,, \quad w = L,T\,, \tag{1}$$

where

$$k_L = \omega\sqrt{\frac{\rho_0}{\kappa_0 + \frac{4}{3}\mu_0}} \quad \text{and} \quad k_T = \omega\sqrt{\frac{\rho_0}{\mu_0}} \tag{2}$$

are the longitudinal and shear wavenumbers in the host material, respectively. According to [8, 11], this dependence is as follows (see Appendix A for more details)

$$\frac{\rho_*(\tilde{\omega})}{\rho_0} = (1-\phi_0)\left[1 + r(\tilde{\omega})\right], \tag{3}$$

$$\frac{\kappa_*(\tilde{\omega})}{\kappa_0} = \frac{4\mu_0(1-\phi_0)}{3\kappa_0\phi_0 + 4\mu_0}\left[1 + k(\tilde{\omega})\right], \tag{4}$$

$$\frac{\mu_*(\tilde{\omega})}{\mu_0} = \frac{1-\phi_0}{1 + \left(1 - \dfrac{3\kappa_0 - 4\mu_0}{9\kappa_0 + 8\mu_0}\right)\phi_0}\left[1 + m(\tilde{\omega})\right], \tag{5}$$

where $r(\tilde{\omega})$, $k(\tilde{\omega})$ and $m(\tilde{\omega})$ are certain complex-valued functions, which tend to zero along with their first derivatives at $\tilde{\omega} = 0$. By a different procedure, the effective material properties were also found by Kuster and Toksöz [1] and are applicable to a dense concentration of voids. The effective bulk and shear moduli, (4) and (5), coincide with either the upper or the lower Hashin-Shtrikman bounds [6].

DOUBLE COMPOSITE MATERIAL

Suppose now that identical ellipsoidal inclusions are distributed randomly and uniformly in the isotropic matrix as pictured in Figure 1. The shape of the ellipsoids is represented by an aspect ratio τ defined by $\tau = a_3 / a_1$ where $a_1 (= a_2)$ and a_3 are the radii along the semi-axes of ellipsoids. Let ϕ_i denote the volume fraction of the ellipsoids. The mass density ρ_*, the bulk modulus κ_*, and the shear stiffness μ_* of the inclusion material are given by Eqs. (3)-(5) in the previous section.

When the ellipsoids are aligned, the wave velocities depend on propagation direction and the coherent waves are in general quasi-longitudinal or quasi-shear. Pure longitudinal waves or pure shear waves can propagate only along directions parallel to the principal axes of ellipsoids. For simplicity we consider here propagation parallel to the principal axes.

Now, if the wavelength of the incident waves is large compared to the size of the ellipsoid, then the field both near the ellipsoid and inside will be essentially quasi-static and uniform.

As discussed in the Introduction, there are various techniques for constructing a homogenized medium to represent the matrix-plus-inclusions composite. The self-consistent method developed in [12] is used to estimate the effective macroscopic elastic constants for the composite material with ellipsoidal inclusions. The predictions of the effective elastic properties are shown to be exactly the same as those derived *via* either Foldy [13] or the Waterman-Truel [7] theories. Links with other homogeneisation schemes and multiple scattering theories (in the low-frequency limit) can be found in [12].

In the following we shall use the tilde sign to non-dimensionalise effective parameters.

We note that the effective inertia of the composite is just the spatial average of the density, *i.e.*,

$$\tilde{\rho} = 1 + (\tilde{\rho}_* - 1)\phi_i = 1 - \phi\,, \tag{6}$$

where ρ and ρ_* are scaled on ρ_0 (*i.e.*, $\rho = \rho_0\tilde{\rho}$, etc.), and ϕ is the porosity determined by

$$\phi = \phi_0\phi_i\,. \tag{7}$$

According to [12], for the case of longitudinal waves propagating in the x_1-direction, a homogeneous material with wavenumber γ_{11} (scaled on k_L) would have the form

$$\tilde{\gamma}_{11}^2 = \tilde{\rho} / \tilde{C}_{11} = \tilde{\rho}(1 - \phi_i\beta_{11})\,, \tag{8}$$

where β_{11} is defined in Eq. (B.9) and

$$\tilde{C}_{11} = (1 - \phi_i\beta_{11})^{-1}\,, \tag{9}$$

is the effective modulus. Similarly, considering propagation in the x_3-direction, we find that

$$\tilde{C}_{33} = (1 - \phi_i\beta_{33})^{-1}\,, \tag{10}$$

where β_{33} is defined in Eq. (B.10). Note that the effective moduli C_{11} and C_{33} are scaled on $\kappa_0 + \frac{4}{3}\mu_0$.

For the case of shear waves polarised in the x_2- and x_3-directions, but propagating in the x_1-direction with effective wavenumbers (scaled on k_T)

$$\tilde{\gamma}_{12}^2 = \tilde{\rho} / \tilde{C}_{66}\,, \quad \tilde{\gamma}_{13}^2 = \tilde{\rho} / \tilde{C}_{55}\,, \tag{11}$$

respectively, we find that

$$\tilde{C}_{66} = \left(1 - \phi_i\beta_{12}\right)^{-1}, \quad \tilde{C}_{55} = \left(1 - \phi_i\beta_{13}\right)^{-1}, \tag{12}$$

where these effective moduli are scaled by μ_0. Coefficients β_{12} and β_{13} are defined in Eq. (B.11). Since the material is transversely isotropic, we can find $\tilde{C}_{12}$ from the expression

$$\tilde{C}_{66} = \tfrac{1}{2}\left(\tilde{C}_{11} - \tilde{C}_{12}\right). \tag{13}$$

Thus, for the transversely isotropic case we have recovered four of the five independent elastic constants in explicit form. In order to obtain $\tilde{C}_{13}$, we require non-normal incidence, which is beyond the scope of this paper.

If τ, ϕ_0 and ϕ_i were all known, it would be straightforward to calculate the velocities of the elastic waves propagating and polarized in the principal directions of the transverse isotropy, *i.e.*,

$$\tilde{v}_{11} = \sqrt{\frac{\tilde{C}_{11}}{\tilde{\rho}}}, \quad \tilde{v}_{33} = \sqrt{\frac{\tilde{C}_{33}}{\tilde{\rho}}}, \quad \tilde{v}_{12} = \sqrt{\frac{\tilde{C}_{66}}{\tilde{\rho}}}, \quad \tilde{v}_{13} = \sqrt{\frac{\tilde{C}_{55}}{\tilde{\rho}}}. \tag{14}$$

Both the density and the stiffness are reduced by the presence of voids. The stiffness decreases at a greater rate than the density, leading to a more significant (and potentially measureable) velocity decrease.

In the following, we apply the double composite model to a notional copper-like material subjected to an intergranular creep process and calculate the effective velocities.

CREEP DAMAGED MATERIAL

Photomicrographic observations of pure copper samples subjected to the intergranular creep process suggest that voids are not randomly positioned [10]. They tend to gather preferentially on the grain boundaries perpendicular to the creep axis. Typically, the void diameter is approximately $10\,\mu$m [9, 10]. The grain shape is nearly equiaxial and the grain size is approximately 0.1 mm [9, 10]. The oriented growth of voids makes the material transversely isotropic around the stress axis.

To predict the effective velocities of materials that have undergone creep, one has to account for the transversely isotropic effective stiffness. We could model any of the following features or a combination thereof: the void shape distribution and orientation.

The damage morphology observed by photomicrograph motivates us to consider a composite modelling relying on the non-random positions of spherical voids. A sketch of this idea is illustrated in Figure 1. Based on these observations, the overall progression of the creep damage can be described as follows. The spherical voids nucleate and grow preferentially on the grain boundaries mostly in areas perpendicular to the applied stress direction. As the creep progresses, the voids form into clusters and the void volume fraction increases. In this paper, the clustered regions are modelled as oblate ellipsoids.

We shall now compare the effective velocities predicted by the double composite model with the experimental results obtained in [14]. This allows us to assess the efficacy of the model.

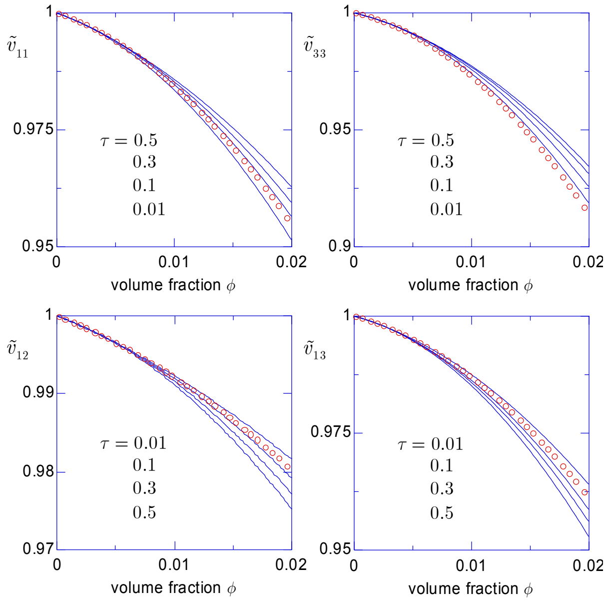

Figure 2. Variation of longitudinal and transverse effective velocities in creep-damaged copper. Solid lines show the predicted velocities for various aspect ratios τ and a constant volume fraction $\phi_i = 0.07$ of oblate-ellipsoidal clusters. The circles represent the results based on the fitting curves of measured velocities presented in [14].

Morishita and Hirao [14] have measured the ultrasonic velocities for pure copper samples subjected to the intergranular creep process. The elastic properties and the density of the polycrystalline copper used for the experimental study [14] are given in Table 1.

Table 1. Material properties of polycrystalline copper.*

ρ_0 (g/cm^3)	μ_0 (GPa)	κ_0 (GPa)
8.98	46.7	136

*Source: (Morishita and Hirao, 1996)

Figure 2 shows the variation of longitudinal and transverse velocities, for both the axial direction x_3 and the radial direction x_1. Circles represent least-square fits of measurement points obtained in [14]. The effective velocities decrease monotonically with increasing porosity ϕ. The agreement between the predictions and measurements is best when the oblate-ellipsoid volume fraction ϕ_i is about 0.07. Except for longitudinal velocity $\tilde{v}_{33}$, all other measured velocities lie between predictions corresponding to oblate ellipsoids of aspect ratio $\tau = 0.01$ and $\tau = 0.1$.

From Figure 2, we see a satisfactory agreement for the four velocities over the whole creep life (*i.e.* wide range of different volume fractions). Therefore, the double composite model is appropriate and is capable of explaining the void-velocity relationships.

CONCLUSIONS

We considered a double composite model to explain the void-velocity relationships of materials subjected to the intergranular creep process. As creep progresses spherical voids nucleate and grow preferentially on the grain boundaries perpendicular to the applied stress direction. In our model the voids are clustered and the void volume fraction increased. The clustered regions are modelled by oblate ellipsoids. The ellipsoid volume elements are sparsely distributed in the matrix, but they continue to grow in volume, containing more and more voids. This evolution produces an anisotropy increase due to the preferential void formation direction. The double composite model, in which the aspect ratio of oblate-ellipsoidal clusters decreases with the increase of creep damage, gave a satisfactory agreement between the predicted and measured velocities. From the model-measurement comparison, one can estimate the oblate-ellipsoid aspect ratio.

REFERENCES

1 G.T. Kuster and M.N. Toksöz, "Velocity and attenuation of seismic waves in two-phase media. Part I, Theoretical Formulations," *Geophysics* **39**, 587–606 (1974).
2 J.D. Eshelby, "The determination of the elastic field of an ellipsoidal inclusion, and related problems," *Proc. R. Soc. A* **241**, 376–396 (1957).
3 H.-S. Chen and A. Acrivos, "The effective elastic moduli of composite materials containing spherical inclusions at non-dilute concentrations," *Int. J. Solids Struct.* **14**, 349–364 (1978).
4 R. Hill, "A self-consistent mechanics of composite materials," *Int. J. Solids Struct.* **13**, 213–222 (1965).
5 B. Budiansky, "On the elastic moduli of some heterogeneous materials," *Int. J. Solids Struct.* **13**, 223–227 (1965).
6 Z. Hashin and S. Shtrikman, "A variational approach to the theory of the elastic behaviour of multiphase materials," *J. Mech. Phys. Solids* **11**, 127–140 (1963).
7 P.C. Waterman and R. Truell, "Multiple scattering of waves*," J. Math. Phys*. **2**, 512–537 (1961).
8 V.K. Varadan, Y. Ma and V.V. Varadan, "A multiple scattering theory for elastic wave propagation in discrete random media," *J. Acoust. Soc. Amer.* **77**, 375–385 (1985).
9 H.M. Ledbetter, R.J. Fields and S.K. Datta, "Creep cavities in copper: An ultrasonic-velocity and composite-modeling study," *Acta metall.* **35**, 2393–2398 (1987).
10 H. Jeong and D.H. Kim, "A progressive damage model for ultrasonic velocity change caused by creep voids in copper," *Mat. Sci. Eng. A* **337**, 82–87 (2002).
11 A.K. Mal and S.K. Bose, "Dynamic elastic moduli of a suspension of imperfectly bonded spheres," *Proc. Camb. Phil. Soc.* **76**, 587–600 (1974).
12 W.J. Parnell, I.D. Abrahams and P.R. Brazier-Smith, "Effective properties of a composite half-space: Exploring the relationship between homogenization and multiple-scattering theories," *Q J Mechanics Appl. Math.* **63**, 145–175 (2010).
13 L.L. Foldy, "Multiple scattering theory of waves," *Phys. Rev.* **67**, 107–119 (1945).
14 T. Morishita and M. Hirao, "Creep damage modeling based on ultrasonic velocities in copper," *Int. J. Solids Struct.* **34**, 1169–1182 (1996).
15 A.N. Norris, "Scattering of elastic waves by spherical inclusions with applications to low frequency wave propagation in composites," *Int. J. Engng Sci.* **24**, 1271–1282 (1986).
16 M. Caleap, B.W. Drinkwater and P.D Wilcox, "Effective wavenumber for coherent elastic wave propagation in media with randomly distributed spheres," *in progress*.
17 C. Zhang and D. Gross, "Wave attenuation and dispersion in randomly cracked solids–I. Slit cracks," *Int. J. Engng Sci.* **31**, 383–399 (1993).
18 T. Mura, *Micromechanics of Defects in Solids* (Kluwer, Dordrecht, 1991).

APPENDIX A

The single sphere problem

Let us consider the scattered fields from a spherical cavity in an isotropic host phase. We consider a spherical polar coordinate system (r,θ,φ) centered at the origin of the sphere and associate with these directions the three unit vectors $\mathbf{e}_r$, $\mathbf{e}_\theta$ and $\mathbf{e}_\varphi$. This polar coordinate system is related to Cartesian coordinates by the relationships $x_1 = r\sin\theta\cos\varphi$, $x_2 = r\sin\theta\sin\varphi$ and $x_3 = r\cos\theta$. Given an incident longitudinal wave of unit amplitude propagating in the positive x_3-direction, in the low-frequency limit, the scattered displacement in the far field is of the form [15]

$$\mathbf{u}^{sc} \underset{r\to\infty}{\sim} A_L^L(\theta)\frac{\mathrm{e}^{\mathrm{i}k_L r}}{k_L r}\mathbf{e}_r + A_T^L(\theta)\frac{\mathrm{e}^{\mathrm{i}k_T r}}{k_T r}\mathbf{e}_\theta, \tag{A.1}$$

where

$$A_L^L(\theta) \simeq \tfrac{1}{3}\tilde{\omega}_L^3\Big(\mathcal{P} + \mathcal{Q}\Big(1-\tfrac{3}{2}\sin^2\theta\Big) - \cos\theta\Big), \tag{A.2}$$

$$A_T^L(\theta) \simeq \tfrac{1}{3}\tilde{\omega}_L^3\big(1-\mathcal{R}\sin\theta\big)\sin\theta, \tag{A.3}$$

and

$$\mathcal{P} = \tfrac{3}{4}\frac{\kappa_0}{\mu_0}, \quad \mathcal{Q} = \frac{20\mu_0}{9\kappa_0 + 8\mu_0}, \quad \mathcal{R} = \tfrac{3}{4}\frac{k_T^2}{k_L^2}\mathcal{Q}. \tag{A.4}$$

If we consider an incident shear wave, polarised in the x_1-direction but propagating in the x_3-direction, we find that the scattered displacement in the far field has the form [15]

$$\mathbf{u}^{sc} \underset{r\to\infty}{\sim} A_L^T(\theta)\frac{\mathrm{e}^{\mathrm{i}k_L r}}{k_L r}\sin\varphi\,\mathbf{e}_r + \mathbf{A}_T^T(\theta,\varphi)\frac{\mathrm{e}^{\mathrm{i}k_T r}}{k_T r}, \tag{A.5}$$

where

$$\mathbf{A}_T^T(\theta,\varphi) = A_{T\theta}^T(\theta)\cos\varphi\,\mathbf{e}_\theta + A_{T\varphi}^T(\theta)\sin\varphi\,\mathbf{e}_\varphi, \tag{A.6}$$

and

$$A_L^T(\theta) \simeq \tfrac{1}{3}\tilde{\omega}_T^3\left(\sin\theta - \tfrac{3}{4}\frac{k_T}{k_L}\mathcal{Q}\sin 2\theta\right), \tag{A.7}$$

$$A_{T\theta}^T(\theta) \simeq -\frac{1}{3}\tilde{\omega}_T^3\big(\cos\theta - \mathcal{R}\cos 2\theta\big), \tag{A.8}$$

$$A_{T\varphi}^T(\theta) \simeq \frac{1}{3}\tilde{\omega}_T^3\big(1+\mathcal{R}\cos\theta\big). \tag{A.9}$$

The scattering dispersion parameter $\tilde{\omega}_w$ is defined in Eq. (1).

The multiple sphere problem

Here, we summarise the predictions of the effective wavenumber obtained using the dispersion relations for the propagation constants of a solid filled with spherical scatterers. From this, we obtain the corresponding effective properties. A comprehensive account of the model derivation can be found in [8, 11] and need not be repeated here. It is sufficient to note that at low frequency, the effective longitudinal and shear wavenumbers are given by

$$\frac{\gamma_L^2}{k_L^2} = \frac{\left(1 - 3\mathrm{i}\phi_0\tilde{A}_0\right)\left(1 - 9\mathrm{i}\phi_0\tilde{A}_1\right)\left(1 - 9\mathrm{i}\phi_0\tilde{A}_2\left(\frac{\kappa_0}{2\mu_0} + 1\right)\right)}{1 + 15\mathrm{i}\phi_0\tilde{A}_2\left(1 - 3\mathrm{i}\phi_0\tilde{A}_0\right) - 9\mathrm{i}\phi_0\tilde{A}_2\left(\frac{\kappa_0}{2\mu_0} + 1\right)}, \tag{A.10}$$

$$\frac{\gamma_T^2}{k_T^2} = \frac{\left(1 - 9\mathrm{i}\phi_0\tilde{A}_1\right)\left(1 - 9\mathrm{i}\phi_0\tilde{A}_2\left(\frac{\kappa_0}{2\mu_0} + 1\right)\right)}{1 + 6\mathrm{i}\phi_0\tilde{A}_2\left(\frac{9\kappa_0}{8\mu_0} + 1\right)}. \tag{A.11}$$

which are identical to the results obtained by Caleap *et al.* [16] if the correlation between scatterers is neglected. Therefore, if the effective mass density is defined as in Eq. (3) and the scattering coefficients $\tilde{A}_j$ given by

$$\tilde{A}_0 = \mathrm{i}\frac{\kappa_0}{\mu_0}, \; \tilde{A}_1 = -\frac{\mathrm{i}}{9} \text{ and } \tilde{A}_2 = \mathrm{i}\frac{4}{3}\frac{\mu_0}{9\kappa_0 + 8\mu_0}, \tag{A.12}$$

then the effective bulk and shear moduli are obtained from the relations

$$\kappa_* + \tfrac{4}{3}\mu_* = \frac{\rho_*\omega^2}{\gamma_L^2} \quad \text{and} \quad \mu_* = \frac{\rho_*\omega^2}{\gamma_T^2}, \tag{A.13}$$

as reported in Eqs. (4) and (5).

Note that the effective wavenumbers (A.10) and (A.11) are the same to $O\left(\phi_0\right)$ as those predicted *via* the Foldy theory (see [17] for an application of this theory). Indeed, the effective wavenumbers are given by

$$\frac{\gamma_L^2}{k_L^2} = 1 + \frac{3\phi_0}{\tilde{\omega}_L^3}A_L^L\left(0\right), \quad \frac{\gamma_T^2}{k_T^2} = 1 + \frac{3\phi_0}{\tilde{\omega}_T^3}A_T^T\left(0\right), \tag{A.14}$$

Upon using Eqs. (A.2) and (A.6) together with the fact that $A_T^T\left(\theta\right) = \mathbf{A}_T^T\left(\theta,0\right)\cdot\mathbf{e}_\theta$, in Eq. (A.14), we find that

$$\frac{\gamma_L^2}{k_L^2} = 1 + \phi_0\left(\mathcal{P} + \mathcal{Q} - 1\right), \quad \frac{\gamma_T^2}{k_T^2} = 1 + \phi_0\left(\mathcal{R} - 1\right), \tag{A.15}$$

which are identical to those derived using a pair-corelation function of hole-correction type in Eqs. (A.10) and (A.11), correct to $O\left(\phi_0\right)$.

APPENDIX B

Eshelby tensor

In the case of ellipsoidal inclusions with semi-axes $a_1 = a_2 \neq a_3$ and aspect ratio $\tau = a_3 / a_1$, the Eshelby tensor is transversely isotropic, defined by the five components (in Voigt's notation) S_{11}, S_{33}, S_{12}, S_{13} and S_{55} (see [18]). They are given explicitly by

$$S_{11} = 3AI_{11} + BI_1, \quad S_{33} = 3AI_{33} + BI_3, \tag{B.1}$$

$$S_{12} = AI_{11} - BI_1, \quad S_{13} = AI_{13} - BI_1, \tag{B.2}$$

$$S_{55} = \tfrac{1}{2}\left[\left(1 + \tau^{-2}\right)AI_{13} + B\left(I_1 + I_3\right)\right], \tag{B.3}$$

where

$$A = \frac{1}{8\pi\left(1 - \nu_0\right)}, \quad B = \left(1 - 2\nu_0\right)A, \tag{B.4}$$

and ν_0 is the Poisson ratio of the host medium. We have also defined

$$I_1 = \frac{2\pi\tau}{1 - \tau^2} \times \begin{cases} \left(\dfrac{\cos^{-1}\tau}{\sqrt{1 - \tau^2}} - \tau\right), & \tau < 1, \\ \left(\dfrac{\cosh^{-1}\tau}{\sqrt{\tau^2 - 1}} - \tau\right), & \tau > 1, \end{cases} \tag{B.5}$$

$$I_3 = 4\pi - 2I_1, \quad I_{33} = \frac{4\pi}{3} - \frac{2\tau^2\left(I_1 - I_3\right)}{3\left(\tau^2 - 1\right)}, \tag{B.6}$$

$$I_{11} = \pi - \frac{I_1 - I_3}{4\left(\tau^2 - 1\right)}, \quad I_{13} = \frac{\tau^2\left(I_1 - I_3\right)}{\tau^2 - 1}. \tag{B.7}$$

Note that when $\tau \to 1$ (spheres), Eqs. (B.5)-(B.7) reduce to

$$I_1 = I_3 = \tfrac{4\pi}{3} \text{ and } I_{11} = I_{33} = I_{13} = \tfrac{4\pi}{5}. \tag{B.8}$$

Coefficients β

We can now define the coefficients β appearing in Eqs. (8)-(10) and (12). One has [12]

$$\beta_{11} = c_\lambda^L\left(2z_1 + z_4\right) + c_\mu^L\left(2z_1 + z_2\right), \tag{B.9}$$

$$\beta_{33} = c_\lambda^L\left(2z_3 + z_6\right) + 2c_\mu^L z_6, \tag{B.10}$$

$$\beta_{12} = c_\mu^T z_2, \quad \beta_{13} = \tfrac{1}{2}c_\mu^T z_5, \tag{B.11}$$

where

$$z_1 = \tfrac{Z_6}{2\Delta}, \quad z_2 = \tfrac{1}{Z_2}, \quad z_3 = -\tfrac{Z_3}{\Delta}, \; z_4 = -\tfrac{Z_4}{\Delta}, \tag{B.12}$$

$$z_5 = \tfrac{4}{Z_5}, \quad z_6 = \tfrac{2Z_1}{\Delta}, \quad \Delta = 2\left(Z_1Z_6 - Z_3Z_4\right), \tag{B.13}$$

and

$$c_\mu^w = \frac{\left(\mu_* - \mu_0\right)k_w^2}{\rho_0\omega^2}, \quad c_\lambda^w = \frac{\left(\kappa_* - \kappa_0\right)k_w^2}{\rho_0\omega^2} - \frac{2}{3}c_\mu^w. \tag{B.14}$$

The subscript w in Eq. (B.14) may refer to either L or T, corresponding to the longitudinal or transverse waves.

The constants Z_j in Eqs. (B.12) and (B.13) are given by

$$Z_1 = \tfrac{1}{2}\left(1 + \left(2a + b\right)\left(S_{11} + S_{12}\right) + 2aS_{13}\right), \tag{B.15}$$

$$Z_3 = Z_4 = a\left(S_{11} + S_{12}\right) + \left(a + b\right)S_{13}, \tag{B.16}$$

$$Z_6 = 1 + 2aS_{13} + \left(a + b\right)S_{33}, \tag{B.17}$$

$$Z_2 = 1 + b\left(S_{11} - S_{12}\right), \quad Z_5 = 2 + 4bS_{55}, \tag{B.18}$$

where

$$a = \frac{\mu_0\kappa_* - \mu_*\kappa_0}{3\mu_0\kappa_0}, \quad b = \frac{\mu_* - \mu_0}{\mu_0}. \tag{B.19}$$